JM3 Journal of Micro/Nanopatterning, Materials, and Metrology

RESEARCH PAPER

E-beam metrology and line local critical dimension uniformity of thin dry resist films for high numerical aperture extreme ultraviolet lithography

Mohamed Zidan,[a,b,*] **Gian Francesco Lorusso**,[b] **Danilo De Simone**,[b] **Anuja De Silva**,[c] **Ali Haider**,[c] **Elisseos Verveniotis**,[c] **Alain Moussa**,[b] and **Stefan De Gendt**[a,b]

[a]KU Leuven, Leuven, Belgium
[b]imec, Leuven, Belgium
[c]Lam Research BVBA, Leuven, Belgium

ABSTRACT. **Background:** Lithography advancements require resist layer thickness reduction, essential to cope with the low depth of focus characteristic of high numerical aperture extreme ultraviolet lithography (High NA EUVL). However, such a requirement poses serious challenges in terms of resist process metrology and characterization, as patterns in thin resist suffer from low contrast, which may affect the performance of the edge detection algorithms used for image analysis, ultimately impacting metrology.

Aim: We aim to investigate the impact of reducing the film thickness of the dry photoresist on the E-beam metrology and line local critical dimension uniformity (LCDU).

Approach: Thin dry resist films from 10 to 30 nm are patterned at pitches 24, 28, and 32 nm using EUVL. A standard critical dimension scanning electron microscope (CDSEM) is used to perform E-beam metrology. The captured SEM images are analyzed using software to extract the parameters of interest, such as the critical dimension (CD), power spectral density (PSD), unbiased line width roughness (uLWR), LWR correlation length, signal-to-noise ratio (SNR), and line LCDU for a range of features with lengths from 12 to 50 nm. Furthermore, the experimental results of the line LCDU of a range of feature lengths and roughness parameters are plotted for different process conditions of thickness and pitch in a normalized way.

Results: The results indicate that the dry resist shows good CDSEM imaging contrast and high SNR even at the thinnest resist thickness. This enables extracting a reliable uLWR measurement without the need to increase the number of frames to modulate the SNR. Moreover, it has LWR correlation length of around 2.5 nm. By thinning the resist thickness, the uLWR and line LCDU increase, and the SNR and the LWR correlation length decrease. Finally, when normalizing the line LCDU to uLWR and the feature length to the correlation length, the resulting curves of the different process conditions of the thickness and pitch overlap with each other, following an analytical model that relates the line LCDU to the resist roughness parameters.

Conclusion: We showed the impact of reducing the dry resist thickness on E-beam metrology and line LCDU for features foreseen for High NA EUVL. The dry resist has good imaging contrast, LWR correlation length of around 2.5 nm, and the line LCDU depends on the resist thickness (uLWR and LWR correlation length for each particular thickness). With such a dataset, we demonstrated an overlap between the normalized curves of the line LCDU to the uLWR and the feature length to the

*Address all correspondence to Mohamed Zidan, Mohamed.Zidan@imec.be

2708-8340/2023/$28.00 © 2023 SPIE

correlation length for the different process conditions of thickness and pitch. The uLWR and correlation length are the knobs to achieve good patterning uniformity for a given feature length.

© 2023 Society of Photo-Optical Instrumentation Engineers (SPIE) [DOI: 10.1117/1.JMM.22.4.044001]

Keywords: thin resist; dry resist; high numerical aperture extreme ultraviolet lithography; E-beam metrology; line local critical dimension uniformity; line width roughness; correlation length

Paper 23058G received Jul. 21, 2023; revised Oct. 24, 2023; accepted Oct. 26, 2023; published Nov. 17, 2023.

1 Introduction

High numerical aperture extreme ultraviolet lithography (High NA EUVL) is a key enabler to extend the semiconductor roadmap to future technology nodes. For such technology node scaling and dense integration, a smaller device footprint is sought after. The critical features are to be patterned with tighter pitches, smaller segment lengths, and good uniformity. Moreover, implementing High NA EUVL necessitates using a thin photoresist because of the limited depth of focus (DOF) and to prevent pattern collapse. As a result, a lithographic feature with High NA EUVL is scaled in three dimensions, as illustrated in Fig. 1(a).

Extensive photoresist materials and metrology development is required to serve such an ecosystem for High NA EUVL. Dry deposited and dry developed photoresist has been introduced that uses closely spaced and small metal-organic units, which reduce resist blurring and increase sensitivity.[1] Furthermore, different process conditions, such as postexposure bake (PEB), dry development, and etch have been optimized to improve its patterning performance toward High NA EUVL.[2] On the other hand, metrology challenges have previously impacted thinner resists below 30 nm when using the existing best-known methods (BKM) for the critical dimension scanning electron microscope (CDSEM). Thinner resist showed limited SEM imaging contrast and decreased signal-to-noise ratio (SNR). This impacts the metrology for the different measurements extraction, such as critical dimension and line roughness.[3] Reliable metrology goes hand in hand with materials for achieving optimized processes development.

The International Roadmap for Devices and Systems (IRDS) specifies the requirements for dimensions of different device architectures and photoresist patterning performance. Future technology nodes target pitches between 16 and 24 nm with a short range of feature lengths.[4] The figures of merit of a resist are low roughness, low dose, and good uniformity. However, it is not enough to use only the standard deviation of the edge position as a metric to screen resists based on the roughness value, frequency analysis characterizing the spread of variation across the feature length is needed. The power spectral density (PSD) analysis is typically done to fully characterize the roughness for a lithographic feature. The standard deviation, correlation length, and

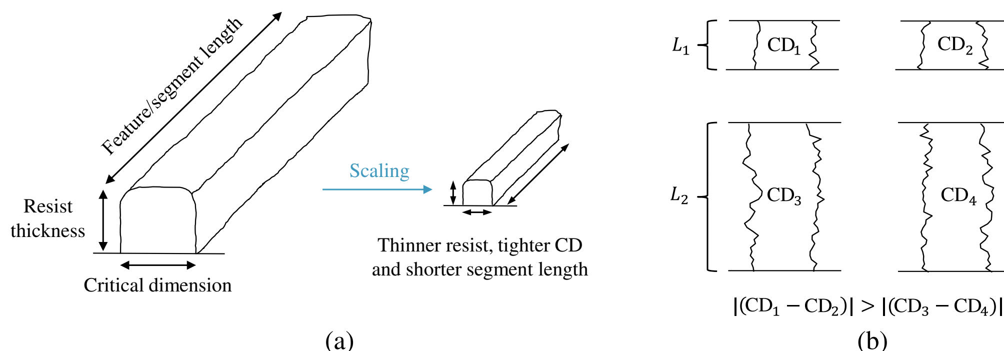

Fig. 1 (a) Illustration of a lithographic feature scaled down for High NA EUVL; thin resist thickness: below 30 nm (a requirement for the limited DOF and preventing pattern collapse), tighter CD: 8 nm, and shorter segment length (for dense integration). (b) Feature-to-feature critical dimension variations dependence on the segment length: shorter segment lengths exhibit larger variations.

roughness exponents (σ, ξ, and α) are the three parameters to completely represent feature roughness.[5]

Those roughness parameters can further describe the mean linewidth variation for features with finite segmented lengths (such as a transistor gate, fin lengths, or any other features with a certain length) patterned with a lithography process, as illustrated in Fig. 1(b). Such variation is typically known as line local critical dimension uniformity (LCDU), which represents the variations in the mean linewidth between one feature to another caused by stochastics.[6,7] A lower line LCDU value is typically preferred.

Line LCDU depends on the resist roughness parameters. Lorusso et al.[8] derived an analytical model relating the line LCDU (σ_{LCDU}) for a feature or segment length (L) to the unbiased line width roughness (uLWR) (σ_{LWR}) and correlation length (ξ) for the case of $\alpha = 0.5$, as shown in Eq. (1). The model was then empirically adjusted by a factor in terms of the roughness exponent in the case of $\alpha \neq 0.5$, as shown in Eq. (2).[9] For a given length, smaller resist roughness and correlation length are advantageous for achieving lower line LCDU. There is a direct proportionality between line LCDU and the roughness: reducing the roughness leads to smaller line LCDU. Additionally, scaling the feature length to smaller values worsens the line LCDU.

For $\alpha = 0.5$, the line LCDU is analytically derived:[8]

$$\sigma_{\mathrm{LCDU}}^2 = \frac{2\xi\sigma_{\mathrm{LWR}}^2}{L}\left[1 - \frac{\xi}{L}(1 - e^{-L/\xi})\right]. \tag{1}$$

For $\alpha \neq 0.5$, the line LCDU is empirically adjusted:[9]

$$\sigma_{\mathrm{LCDU}}^2 = \frac{(2\alpha + 1)\xi\sigma_{\mathrm{LWR}}^2}{L}\left[1 - \frac{\xi}{L}(1 - e^{-L/\xi})\right]. \tag{2}$$

We can gain additional insights considering this model as it relates those fundamental resist roughness parameters to the feature-to-feature line LCDU for a specific physical feature length. When scaling from one technology node to another, feature lengths are expected to shrink and will eventually approach the correlation length values. Taking the mathematical limit of Eq. (1), when $L \to \xi$, then σ_{LCDU} is equal to $\sqrt{2/e}\sigma_{\mathrm{LWR}} \approx 0.86\sigma_{\mathrm{LWR}}$. As a result, a smaller correlation length allows to pattern features with line LCDU values below this 0.86 σ_{LWR} limit. Moreover, Mack[9] utilized numerical simulations to generate random rough features with a range of roughness and correlation lengths fixing α at 0.5 to calculate the resulting line LCDU. When normalizing the line LCDU to the uLWR and the segment length to the correlation length, the resulting curves overlap with each other and match the analytical expression of Eq. (1) until $L \geq 3\xi$. Biases when generating small rough lines diverged the simulations for $L \leq 3\xi$.[9] Experimental investigation of such overlap between the normalized curves of line LCDU to uLWR and segment length to correlation length for different processes and comparison to the above analytical model is still missing.

In this work, we will first study the SEM image visibility, SNR, uLWR BKM for the thin dry resist from 10 to 30 nm at pitches 24, 28, and 32 nm. Additionally, to the best of our knowledge, no one has investigated the impact of reducing the film thickness on LWR correlation length and line LCDU for such feature lengths targeted by High NA EUVL. The rest of the manuscript will focus on the uLWR, LWR correlation length, and line LCDU for those specific feature lengths at pitches 24 and 28 nm for the thin resist. Finally, given the design of experiment of different pitches, roughness, and correlation lengths for this resist, we can investigate the experimental and analytical trends when constructing normalized curves between line LCDU to uLWR and segment length to correlation length for those different process conditions of thickness and pitches.

2 Experiment

2.1 Wafer Stack and Materials

In this study, a negative tone dry resist is deposited using chemical vapor deposition at five resist thicknesses (nominally deposited at those thicknesses 10, 15, 20, 25, and 30 nm) on a baseline underlayer. 1:1 line and space with pitch 24, 28, and 32 nm are targeted. The process parameters,

such as deposition, PEB, and dry development, are tuned for pitch 24 and 28 nm. The exposure is done using NXE 3400 ASML EUV scanner, with a reticle for pitch 32 and another reticle for pitches 24 and 28 nm. The illumination was done using three dipole sources with different sigma depending on the pitch. The normalized image log slope (NILS) values for these features are 2.53 for P24, 2.70 for P28, and 2.25 for P32. These values were derived from simulations that took into account the sources used and a 60 nm Ta-based mask with 0.3 nm Ru overetch.[10] Flare was set to 4%, assuming that average mask transmission is the same as for the line and space clip. For P24, it is the maximum achievable NILS with 0.33 NA, whereas for P32, the NILS could be improved using a different source.

2.2 Measurement Conditions and Analysis

Hitachi CDSEM CG6300 captures images using the imec LWR BKM conditions.[11] The landing energy is set at 500 eV. Other SEM parameters are kept fixed, such as the probe current: 8 pA, pixel size: 0.8 nm, number of pixels: 2048×2048, and magnification: 82.4 k. With such settings, the field of view is $1.638 \times 1.638\,\mu\text{m}^2$. First, for pitch 32 nm, the number of frames of integration is varied from 1 frame to 64 frames to find the number of frames required to reach the plateau of the roughness.[12] Second, for pitches 24 and 28 nm, 16 frames are used, because 16 frames are found to be a reliable setting, as it will be explained below. A total of 50 images per condition is measured. Fractilia MetroLER is used to analyze all the images and extract the different measurements such as the mean CD, SNR, unbiased line width roughness, LWR correlation length, and PSD. The line LCDU per each CD segment length is calculated as follows: the segment length can be specified as an input in MetroLER as the "length for low frequency," and to get the line LCDU per each CD segment length, the "local line segment CDU" output from the software is extracted. A range of lengths from 12 to 50 nm is applied to calculate their corresponding line LCDU and distribution for the different resist thicknesses and pitches. Additionally, Park atomic force microscope (AFM) NX Series is used to measure the actual film thickness after the dry development step.

3 Results and Discussion

3.1 AFM Measurement

Resist array height after dry development is measured using an AFM. AFM images are acquired with resolution of 2048 pixels in 64 lines and contain empty areas and array of resist lines and spaces, as shown in Fig. 2. The data within the colored rectangles are averaged to get the cross sections in Fig. 3. The array height is extracted by subtracting the height of the area with the array of lines from the height of the empty areas as shown in the cross sections image. Figure 4 shows the measured AFM resist array height versus the nominally deposited film thickness. Upon dry development, the resist height reduces by 50% to 30%. The slopes for each pitch are not significantly different; P32: 0.58 ± 0.018, P28: 0.63 ± 0.014, and P24: 0.57 ± 0.004.

3.2 SEM Image Visibility Using imec BKM Conditions

A visual comparison of the SEM images of the different film thicknesses and pitches is shown in Fig. 5 using the imec LWR conditions of 16 frames of integration. It is observed that there is good imaging contrast between the resist and underlayer, even at the thinnest film thickness of 10 nm

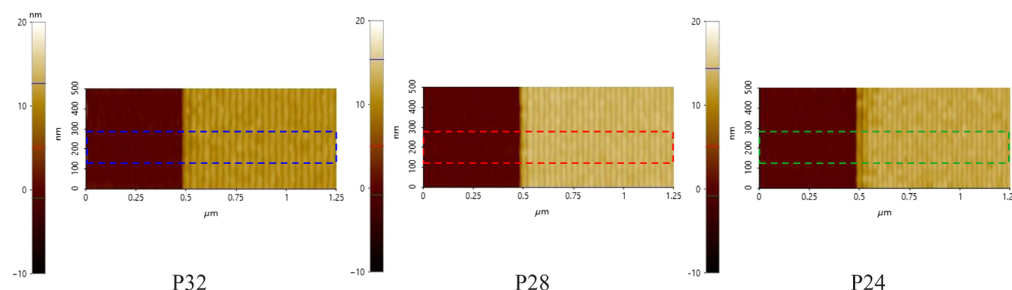

Fig. 2 AFM captured images containing empty areas and array of line and spaces for the three pitches of 20 nm nominal film thickness.

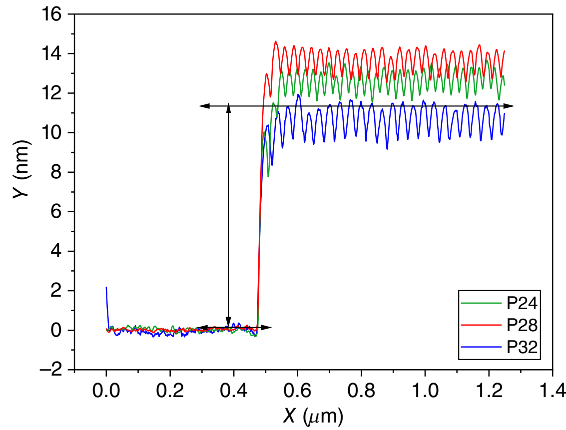

Fig. 3 AFM cross sections of the data averaged within the colored rectangles in Fig. 3.

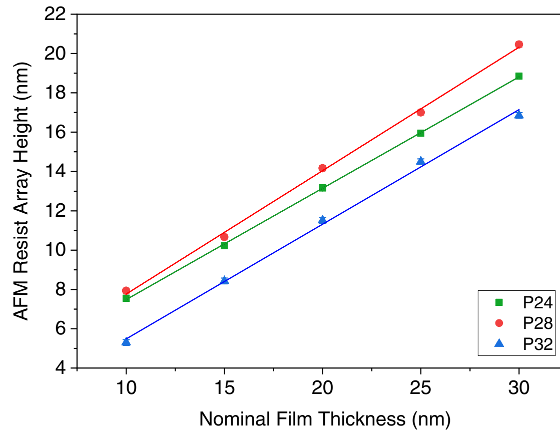

Fig. 4 AFM resist array height after dry development step for the different nominally deposited film thickness. The error bars on the data are contained in the size of the symbol. The resist height reduces by 50% to 30% after dry development step. Figure was previously published in Ref. 13.

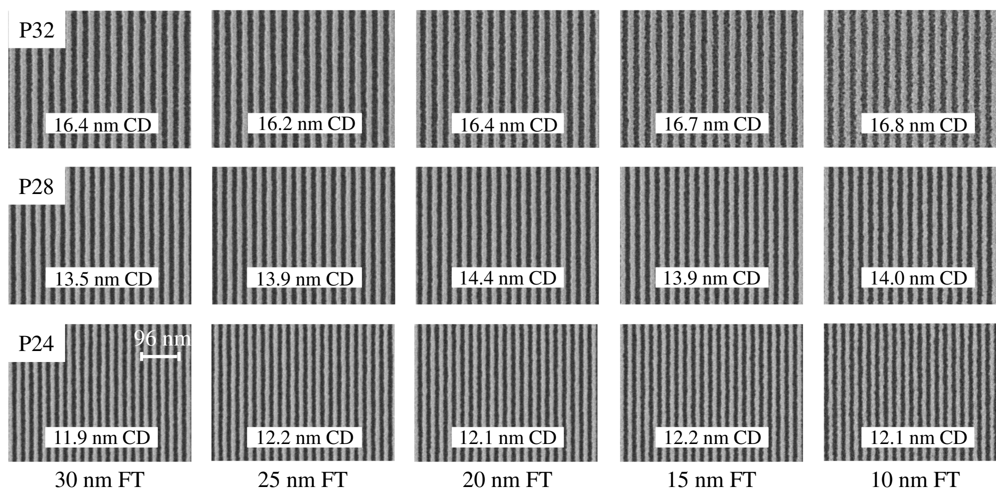

Fig. 5 SEM images for thin dry resist thicknesses of 10 to 30 nm FT at pitches 24, 28, and 32 nm. Within-target mean CD is added for each corresponding resist thickness and pitch. Figure was previously published in Ref. 13.

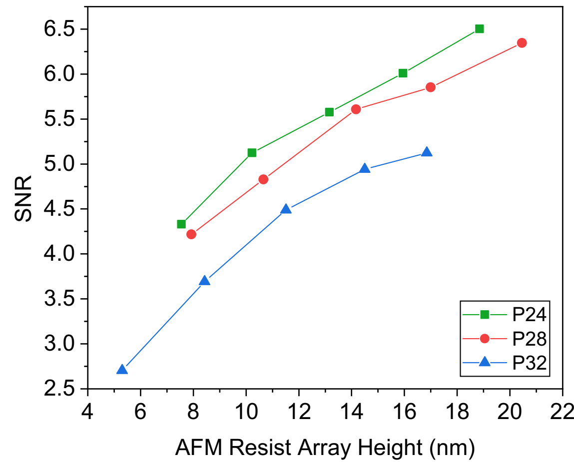

Fig. 6 SNR as a function of the resist thickness using 16 frames. SNR values are above 2 for all the resist thicknesses. Thinning resist thickness decreases the SNR as expected. Figure was previously published in Ref. 13.

for the three pitches. Considering the SNR values, Fig. 6 shows that the SNR values are above 2, which is the threshold defined for reliable metrology.[12,14] Moreover, the SNR decreases with reducing the film thickness as expected and reported for other types of resists.[3,12]

3.3 Roughness Parameter Extraction

Thin CAR below 30 nm has previously faced metrology challenges due to the limited SNR, which impacts the uLWR measurements extraction. The uLWR estimate becomes artificially low at small SNR values (below 2) and reaches a reliable plateau value at high SNR.[12] The methodology is that the frames of integration are varied to modulate the SNR until this plateau is reached, and then the corresponding number of frames can be used as a reliable metrology setting for that type of resist. In Fig. 7, the number of frames is varied from 1 to 64 frames of integration to observe the uLWR trend with the SNR for such stack at pitch 32 nm. uLWR estimate is observed to improve by increasing the SNR. 16 frames of integration are enough for reaching the plateau and achieving reliable roughness values for the thin dry resist, even at 10 nm FT. With such SNR reported in Fig. 6, this encourages measuring the LWR using 16 frames for investigating this resist and underlayer stack at tighter pitches of 28 and 24 nm for the rest of this work.

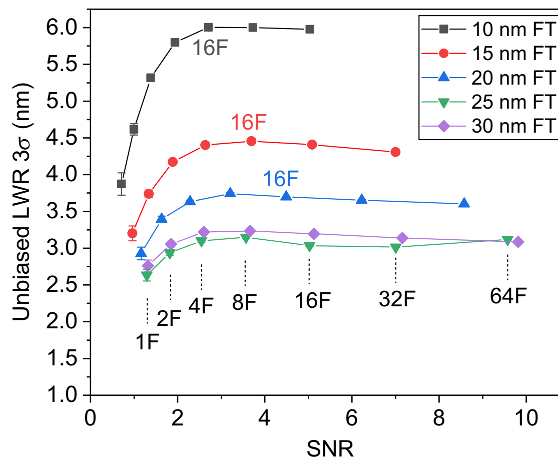

Fig. 7 uLWR trend with the SNR for the different resist thicknesses at pitch 32, the SNR is modulated by varying the number of frames of integration at the CDSEM. The uLWR reaches a plateau after 16 frames for all the resist thicknesses, indicating a reliable measurement using the current imec LWR BKM for this resist. Figure was previously published in Ref. 13.

Applying such metrology BKM for pitch 24 and 28 nm, at the same resist thickness range, the uLWR for P24 and P28 are 21% to 35% reduced compared to P32. This reduction can be attributed to the elevated NILS values resulting from the selected exposure sources, combined with process optimization for P28 and P24. Figure 8 illustrates the uLWR and the LWR correlation length for the five resist thicknesses for P24 and P28. By thinning the resist thickness, the roughness increases because of the increased stochastics: a lower exposure dose is required for thin resists, which increases the variability of the absorbed photons within a volume. Moreover, thinner resists have less vertical averaging of the top-down line profile during SEM imaging, so they appear rougher. The correlation length values are around 2.5 nm, which is considered small since this resist is composed of small metal-organic clusters. The small correlation length indicates small resist blur and the correlation mechanisms occurring at a shorter distance scale than the conventional CAR. Moreover, with thinning the resist, the correlation length decreases. This can be further visualized using the PSD for the different resist thicknesses. Figure 9 plots the biased and unbiased PSD curves for the different resist thicknesses at pitch 24. By reducing the film thickness, the PSD(0) increases, and there is this shift in the correlation length to smaller lengths.

Furthermore, considering both parameters shown in Fig. 8, exponential fitting has been applied to capture the parameters' dependence on the resist thickness (T). The goodness of fit ranges from 0.96 to 0.99. With thinning the resist thickness, uLWR rates of increase are 0.19 ± 0.042 and 0.246 ± 0.055, whereas the correlation length rate of decrease is 0.137 ± 0.079 and 0.128 ± 0.063 for P28 and P24, respectively.

Line wiggling, extracted from MetroLER, is further plotted with the line aspect ratio (AFM array height divided by the CDSEM mean CD) in Fig. 10. As anticipated, there is an increase in

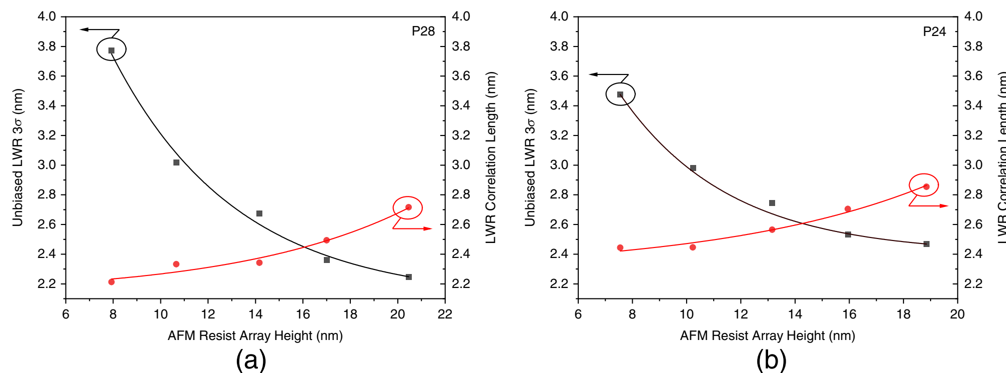

Fig. 8 Impact of thinning the resist thickness on the uLWR and the LWR correlation length for pitch (a) 28 nm and (b) 24 nm. The roughness increases, and the correlation length decreases by thinning the resist. The error bars on the data are contained in the size of the symbol, ranging from 0.004 to 0.012 nm.

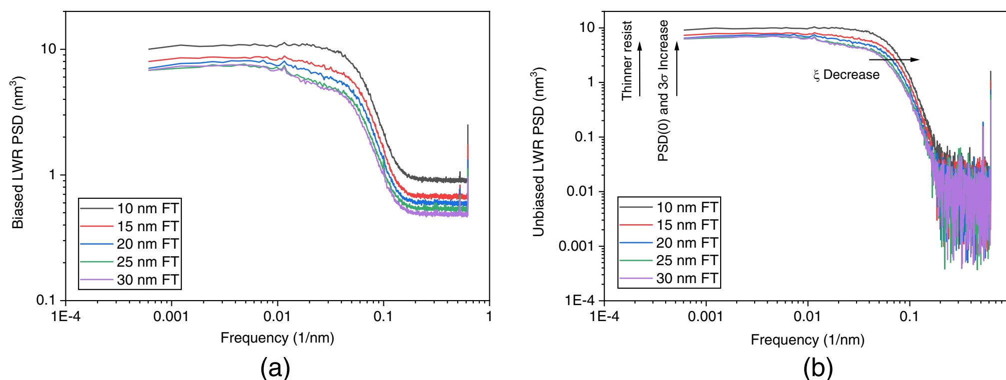

Fig. 9 (a) Biased and (b) unbiased LWR PSD for the different resist thicknesses at pitch 24. Thinning the resist thickness leads to an increase in the PSD(0) and root-mean-square value, additionally, the correlation length decreases.

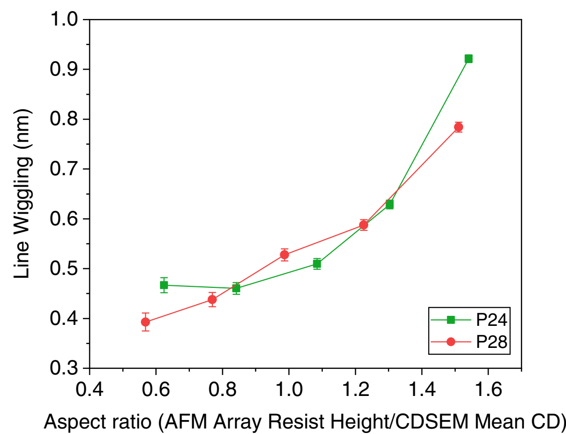

Fig. 10 Line wiggling plot with the line aspect ratio of P24 and P28 features. The line wiggling increases with a higher line aspect ratio as expected.

line wiggling with a higher line aspect ratio. However, the images do not exhibit pattern collapse at the optimal dose and focus, as illustrated in Fig. 5.

3.4 Line Local Critical Dimension Uniformity

Features patterned using High NA EUVL will be scaled in thickness, pitch, and their lengths. Certain devices will even require stringent feature lengths down to 12 nm with good uniformity.[4] This range of lengths will start approaching the resist roughness correlation lengths, which worsens feature-to-feature uniformity. The line LCDU for a given segment length depends on uLWR, and correlation length, as explained in the analytical model of Eq. (1). As a result, resist screening activities need to consider both the uLWR and correlation length. Smaller uLWR and correlation lengths are advantageous to minimize the line LCDU.

For the dry resist, the line LCDU dependence on the segment length for the different resist thicknesses for pitch 28 and 24 is plotted in Figs. 11(a) and 11(b). The corresponding uLWR and LWR correlation length are added to the legend for each resist thickness. The line LCDU ranges between 1 and 2.8 nm depending on the resist thickness and feature length. It is observed that the whole curve shifts upward by reducing the film thickness. So thinning the resist leads to larger line LCDU since thinner resists have larger roughness. Line LCDU is worse for shorter segment lengths, as expected.

Furthermore, we can consider the CD distribution for the different segment lengths. (The line LCDU values reported in Fig. 11 are three times the standard deviation of the CD distributions.) Figure 12(a) shows the distribution of the mean CD of a resist thickness of 25 nm for those various segment lengths at pitch 24. The distribution variance of smaller segment lengths is

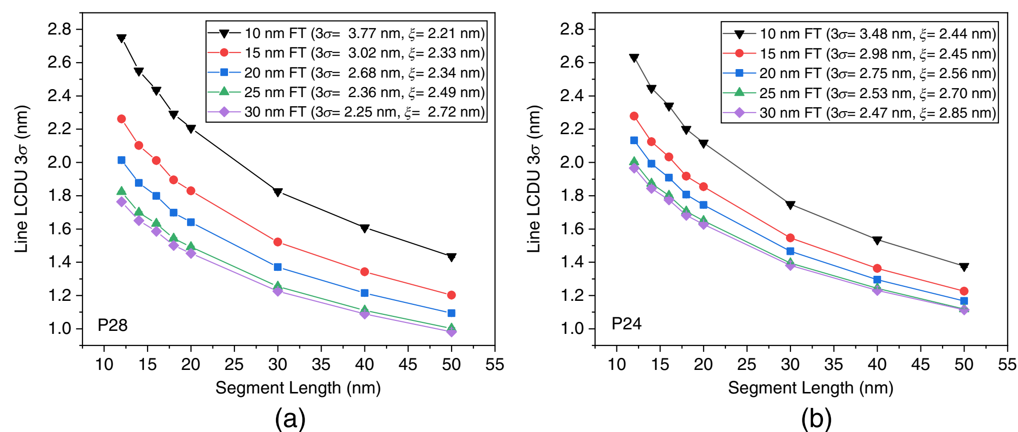

Fig. 11 Line LCDU of certain segment lengths for different resist thicknesses at (a) pitch 28 nm and (b) 24 nm. Thin resist thickness and short feature length exhibit larger line LCDU.

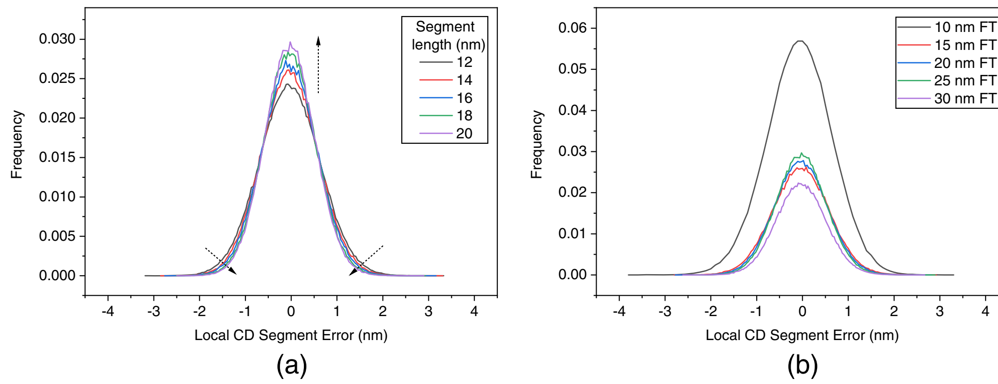

Fig. 12 (a) CD distribution of the different segment lengths for a resist thickness of 25 nm at pitch 24 nm. (b) CD distribution of 20 nm segment length for different resist thicknesses at pitch 24 nm. CD distribution variance increases with smaller segments and thinner resists.

larger compared to longer segment lengths (0.30 for 20 nm segment versus 0.44 for 12 nm segment). Figure 12(b) shows the impact of reducing the film thickness on the CD distribution for a 20 nm segment length at pitch 24 nm. Segments patterned with 10 nm FT will have a larger variability than those patterned with thicker resist thickness. Therefore, devices patterned with thinner resist, shorter gate lengths, and tighter pitches will have larger variability, which is an additional challenge impacting device making using High NA EUVL.

With such available measurements of the line LCDU, uLWR, and correlation lengths for a range of segment lengths of the different resist thicknesses and pitches, we can construct a normalized graph between the line LCDU/uLWR and the segment length/correlation length. Figure 13 shows that those normalized curves overlap with each other, which suggests that the different process conditions of thicknesses and pitches seem to follow a universal trend. Additionally, the model described in Eq. (2) is plotted against the experimental results using α as a single fitting parameter. It is observed that there is a good match between this fitted expression and the experimental results. The fitted α value is 1.26, which agrees with the extracted experimental values of α ranging between 1.32 and 1.98 with an average of 1.64 and standard deviation 3σ of 0.56.

The learning from such universal overlaps between the different processes is that the line LCDU between feature-to-feature will be impacted by the roughness value of the resist depending on the ratio of the feature length to the correlation length. At the rightmost part of the x axis, i.e., for segments that are long enough than the correlation length, the line

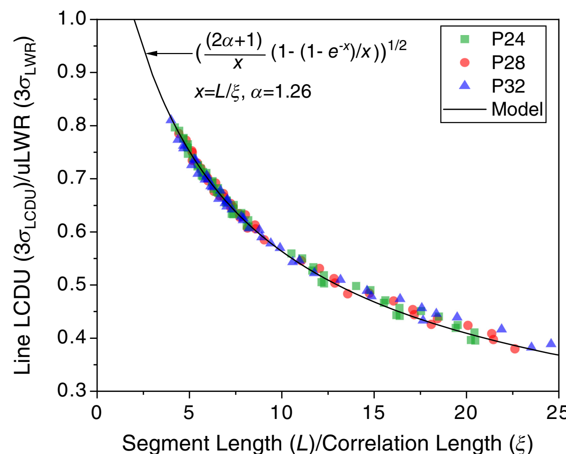

Fig. 13 Normalization of the line LCDU and segment length to the uLWR and correlation length parameters for the different resist thicknesses at pitches 24, 28, and 32. Experimental investigation of such overlapping between the normalized parameters is shown with a good match to the line LCDU model of Eq. (2).

LCDU will be less impacted by the uLWR. At the leftmost part of the x axis, when the segment length approaches the correlation length, the line LCDU approaches the uLWR. In other words, the uLWR controls the largest values of the line LCDU, whereas the correlation length limits the minimum segment lengths possible for a given line LCDU.

4 Conclusions

Previous studies on the thin CAR below 30 nm showed deteriorated imaging contrast and reduced SNR, which posed an E-beam metrology challenge. However, this is not the case for all the thin resist and underlayer combinations. This study investigated thin dry resist from 10 to 30 nm at pitches 24, 28, and 32 nm. The stack showed good imaging contrast, even for 10 nm thickness. Additionally, the roughness BKM using 16 frames is suitable enough for reliable roughness extraction (uLWR reaching the plateau at 16 frames).

Considering the patterning parameters, this class of resist has a correlation length of around 2.5 nm depending on the resist thicknesses, which indicates less resist blur. Furthermore, the analysis done on the different resist thicknesses shows an increase in the uLWR and line LCDU, and a decrease in the correlation length and SNR with reducing the resist thickness. Considering the CD distribution of a segment length, scaling down the feature's pitch, length, and thickness will lead to larger variability and wider distributions of their CD, which is a challenge for High NA EUVL.

Finally, with such a dataset, we demonstrated overlapping normalized curves between the line LCDU to the uLWR and the segment length to the correlation length for different process conditions of five thicknesses and three pitches. This sheds light on a wider view to lithographically pattern features with good uniformity. Resist screening activities should consider both the uLWR and correlation length parameters. Smaller uLWR and correlation length enable scaled features to achieve good line LCDU.

Code, Data, and Materials Availability

Company proprietary information will not be made available, but manuscript content is consistent with JM3 technical content guidelines.

Acknowledgments

Part of this manuscript has been previously published in the SPIE Conference Proceedings: Proc. SPIE 12496, Metrology, Inspection, and Process Control XXXVII, 1249612 (27 April 2023) 10.1117/12.2658280.[13] We would like to acknowledge Joern-Holger Franke from imec for the fruitful discussion and calculating the NILS values.

References

1. R. S. Wise, "Breaking stochastic tradeoffs with a dry deposited and dry developed EUV photoresist system," *Proc. SPIE* **11612**, 1161203 (2021).
2. H. S. Suh et al., "Dry resist patterning readiness towards high-NA EUV lithography," *Proc. SPIE* **12498**, 1249803 (2023).
3. G. F. Lorusso et al., "E-beam metrology of thin resist for High NA EUVL," *Jpn. J. Appl. Phys.* **62**, SG0808 (2023).
4. "The International Roadmap for Devices and Systems: lithography," 2022, https://irds.ieee.org/editions/2022/irds%E2%84%A2-2022-lithography.
5. V. Constantoudis et al., "Line edge roughness and critical dimension variation: fractal characterization and comparison using model functions," *J. Vac. Sci. Technol., B: Microelectron. Nanometer Struct. Process., Meas., Phenom.* **22**, 1974–1981 (2004).
6. Y. Ma, H. J. Levinson, and T. Wallow, "Line edge roughness impact on critical dimension variation," *Proc. SPIE* **6518**, 651824 (2007).
7. P. Kruit and S. Steenbrink, "Local critical dimension variation from shot-noise related line edge roughness," *J. Vac. Sci. Technol., B: Microelectron. Nanometer Struct. Process., Meas., Phenom.* **23**, 3033–3036 (2005).
8. G. F. Lorusso et al., "Spectral analysis of line width roughness and its application to immersion lithography," *J. Micro/Nanolithogr. MEMS MOEMS* **5**(3), 033003 (2006).
9. C. A. Mack, "Analytical expression for impact of linewidth roughness on critical dimension uniformity," *J. Micro/Nanolithogr. MEMS MOEMS* **13**(2), 020501 (2014).

10. I. Makhotkin et al., "Refined extreme ultraviolet mask stack model," *J. Opt. Soc. Am., A:* **38**, 498–503 (2021).
11. G. F. Lorusso et al., "The need for LWR metrology standardization: the imec roughness protocol," *Proc. SPIE* **10585**, 105850D (2018).
12. J. Severi et al., "Chemically amplified resist CDSEM metrology exploration for High NA EUV lithography," *J. Micro/Nanopatterning, Mater. Metrol.* **21**(2), 021207 (2022).
13. G. F. Lorusso et al., "Dry resist metrology readiness for high-NA EUVL," *Proc. SPIE* **12496**, 1249612 (2023).
14. C. A. Mack et al., "Unbiased roughness measurements from low signal-to-noise ratio scanning electron microscope images," *J. Micro/Nanopatterning, Mater. Metrol.* **22**(2), 021006 (2022).

Mohamed Zidan received his joint Erasmus Mundus Master of Science degree in nanoscience and nanotechnology from the KU Leuven and TU Dresden and his Bachelor of Science degree in nanotechnology and nanoelectronics engineering from the UST at Zewail City of Science and Technology, Egypt. He is currently a PhD student working on the topic of photoresist metrology and the development for High NA EUV lithography in collaboration between the KU Leuven and the Metrology Group of the Advanced Patterning Department at imec.

Gian Francesco Lorusso received his PhD in solid-state physics from the University of Bari, Italy, in 1992. He has been working on topics related to the semiconductor industry, such as metrology tool development, lithography, and material analysis. His domains of expertise include lithography, metrology, microscopy, and spectrometry. After working at the École Polytechnique Fédérale de Lausanne (Switzerland), the Center for X-ray Lithography (Wisconsin), the Center for X-ray Optics at Lawrence Berkeley National Laboratories (California), and KLA-Tencor (California), he has joined imec (Belgium) in 2006. His work has produced more than 230 papers and 17 patents and was awarded with both the Vladimir Ukraintsev and Diana Nyyssonen Awards. He is working on extreme ultraviolet lithography and metrology, fields in which he started in the early nineties.

Danilo De Simone is a scientific director in the Advanced Patterning Department at imec. He has 23 years of experience in semiconductor R&D field. Before imec, he worked for STMicroelectronics, Numonyx, and Micron, leading the development of lithographic materials for HVM NOR, NAND, and PCM devices. He is an editorial board member of the *Journal of Micro/Nanopatterning, Materials, and Metrology*, a member of SPIE committee for the Patterning Materials and Processes program, and a member of the International Advisory Board of the Photopolymer Science and Technology Conference. He has co-authored more than 140 papers.

Anuja De Silva is a technical director at Lam Research. She has co-authored more than 70 publications on EUV materials and process development. She obtained her PhD from Cornell University. She is a senior member of SPIE.

Ali Haider is a process engineer at Lam Research Organization. He is a member of Dry-Resist Patterning Team at Lam Belgium. He has expertise with vapor phase thin film deposition techniques and authored several publications on atomic layer deposition process development. He received his PhD from Bilkent University in 2017.

Elisseos Verveniotis is a process engineer at Lam Research. He obtained his PhD from Charles University, Prague, Czech Republic.

Alain Moussa received his bachelor's degree in chemistry from Haute École Léonard de Vinci of Bruxelles, Belgium, in 2000. He has worked at the Catholic University of Louvain-La-Neuve in research for polymer synthesis and thin film deposition on silicon as well as their characterization by XRR, AFM, ellipsometry, and SEM. Since 2005, he has joined imec, where he is working in scanning probe microscopy domain, and today, in the metrology department for lithography patterning and process control, as R&D engineer.

Stefan De Gendt is a fellow at imec and a part-time full professor at the Katholieke Universiteit Leuven. He obtained his master's and PhD degrees from the University of Antwerp in 1996 and has since been working at imec in roles related to unit process technology and materials for CMOS technology. He has co-authored more than 500 papers and graduated 25+ PhD students.